JOURNAL OF MATERIALS SCIENCE 3 (1968) 349–359

Self-Diffusion of Ti, Zr, and Hf in their HCP Phases, and Diffusion of Nb^{95} in HCP Zr

F. DYMENT
Consejo Nacional de Investigaciones Científicas y Técnicas, Buenos Aires, Argentina
C. M. LIBANATI
Metallurgy Department, Comisión Nacional de Energía Atómica, Buenos Aires, Argentina

Received 12 February 1968

Preliminary values for the self-diffusion constants of α-(hexagonal cp) Hf and new values for the self-diffusion constants of α-(hcp) Zr are given. A new determination of the latter was considered necessary since existing values disagree widely and the experimental methods employed in their determination are not considered to be sound. Values obtained by the authors for the self-diffusion constants of α-Ti are reviewed.

The activation energies obtained are much smaller than those predicted by relationships based on physical properties of the elements and, within the experimental error, they have similar values to those corresponding to the β-(body-centred cubic) phases. Frequency factors are too small to satisfy Zener's theory; when interpreted according to a vacancy model they give negative activation entropies, and the relationship $D_0(\alpha)/D_0(\beta)$ is approximately the same for the three elements.

It is suggested that the same diffusion mechanism operates in both the α- and β-phases. If two mechanisms operate in the β-phase, the low temperature one is the same as operates in the α-phase.

1. Introduction

Ti, Zr and Hf belong to the IV-A group of the periodic table. They have two phases: the α-phase, hcp, stable at low temperatures and the β-phase, bcc, stable at high temperatures.

A certain deviation from the normal diffusion behaviour [1] has been found for impurity-diffusion and self-diffusion in β-Ti [2-6], β-Zr [7-10], and γ-U [11, 12] and for self-diffusion in β-Hf [2, 13]. Activation energies are much smaller than those predicted by relationships based on physical properties of the elements. Frequency factors are generally too small to satisfy Zener's theory; when interpreted according to a vacancy model they give negative activation entropies.

An unusual feature of certain results [3, 6-8] is that, if diffusion rates are described by an Arrhenius equation $D = D_0 \exp(-Q/RT)$, the apparent activation energy and frequency factor increase with increasing temperature.

There are two possible interpretations of non-linear Arrhenius plots: (i) Q and D_0 are temperature dependent. A single diffusion mechanism would give a curved plot of $\ln D$ versus $1/T$; (ii) at least two distinct diffusion processes occur simultaneously with different but constant activation parameters.

There has been considerable speculation concerning operative diffusion mechanisms [1, 5, 8, 14-16] but, up to now, no theory has been sufficiently proved. One of the attempts to explain the anomalous behaviour of certain elements assumes that volume-diffusion measurements are enhanced by randomly distributed dislocations which constitute short circuits for diffusing atoms. The contribution of dislocations to diffusion has been investigated by Hart [17] and Mortlock [18] and applied to impurity diffusion in β-Ti and β-Zr by Le Claire [1] and Kidson [14]. Naik and Agarwala [19] applied the same theory to impurity-diffusion and self-diffusion in α-Zr. By a quantitative treatment they explained the enhancement of apparent volume-diffusivity as resulting from randomly distributed dislocations with a density of $10^7/cm^2$. We do not consider that treatment to be entirely satisfactory [20].

The problem has been generally considered mainly from the structural point of view, probably owing to the fact that, with the exception of some work on α-Zr [21-24] with widely scattered results and our own work on α-Ti [25], all the anomalies have been found in the bcc phase [2-13].

The volume self-diffusion of Ti, Zr, and Hf in the α-(hcp) phase are studied here, trying to elucidate whether or not the anomalies are exclusive to the bcc β-phase or if they also appear in the α-phase.

Despite previous investigations, α-Zr has also been included because of the high disagreement among existing values and the fact that, with one exception, the influence of Nb^{95} in the tracer was not considered. Zr^{95} decays to radioactive Nb^{95}, which in turn decays to stable Mo^{95}. A NaI (Tl) crystal is unable to resolve the very proximate gamma radiation energies emitted by both isobars (table I) and it is difficult to attain secular equilibrium conditions in a reasonable time since their half-lives are of similar magnitude: 65 days for Zr^{95} and 35 days for Nb^{95}. Therefore, and even assuming that previous determinations were carried out with Zr^{95} initially free from Nb^{95}, there was a reasonable amount of it present in the specimen even after the shortest of the annealing treatments.

TABLE I

Radioisotope	Zr^{95}			
Half-life	65 days			
Production	Zr^{94} (n, γ) Zr^{95}			
Decay	Zr^{95} ⇓	$\xrightarrow[65\ \mathrm{days}]{\beta^-}$	Nb^{95} ⇓	$\xrightarrow[35\ \mathrm{days}]{\beta^-}$ Mo^{95}
Radiation emitted	β	γ	β	γ
Energy (MeV)	0.36	0.726	0.16	0.765
	0.40	0.760		
	0.89			

The effect of Nb^{95} was taken into account by Flubacher [24] who after sufficiently long annealing periods was able to apply the direct sectioning method. Reportedly up to 90% of Nb^{95} was then chemically eliminated from the sectioned material (before activity measurements). One of the three qualities of Zr employed was stabilised in the α-phase; the remaining two, non-stabilised, showed considerable grain growth. This may account for the wide scattering of D values obtained. Single values of Q and D_0 were calculated from the three sets of specimens.

In the present work, 99.99 wt % Zr, grain-stabilised in the α-phase, was used. Radiations from Zr^{95} and Nb^{95} were separated using a Ge/Li semi-conductor detector. The diffusion constants for Nb^{95} in α-Zr were also determined in order to evaluate its influence in the above-mentioned measurement.

Our results show that the self-diffusion anomalous behaviour is characteristic of *both* phases of this group of metals.

2. Experimental Method

The diffusion coefficients were calculated by Seibel's generalisation [26] of Gruzin's method [27]. This is a combination of the sectioning and absorption techniques, as the residual activity of the specimen is measured after each sectioning. This requires a knowledge of the absorption coefficient for the radiation being used. However, for extreme cases, i.e. highly and slightly absorbed radiation, simple solutions, which do not involve the absorption coefficient, exist for Fick's equations.

The solution for slightly absorbed radiation has been integrated and, as in the direct sectioning method, it is possible to work directly with the experimental data by plotting activity versus penetration in a gauss-arithmetic graph.

The solution of Fick's second law for a semi-infinite medium with a thin layer of radioisotope located on the planar surface at $t = 0$, is by Gruzin's method

$$\mu A_n - \frac{\partial A_n}{\partial x_n} = \frac{k\,M}{\sqrt{\pi D t}} \exp\left(-\frac{x_n^2}{4\,Dt}\right) \qquad (1)$$

where μ = linear absorption coefficient; A_n = activity of the specimen after a total thickness x_n has been sectioned; D = diffusion coefficient; t = diffusion-annealing time.

For slightly absorbed radiation, equation 1 reduces to

$$-\frac{\partial A_n}{\partial x_n} = \frac{k\,M}{\sqrt{\pi D t}} \exp\left(-\frac{x_n^2}{4\,Dt}\right) \qquad (2)$$

and integrating between $0 \leqslant x_n \leqslant \infty$

$$A_n = A_0 \left[1 + \mathrm{erf}\left(-\frac{x_n}{4\,Dt}\right)\right] \tag{3}$$

where

$$\mathrm{erf}\,(u) = \frac{2}{\sqrt{\pi}} \cdot \int_0^u \mathrm{e}^{-t^2}\,\mathrm{d}t \tag{4}$$

is the error function.

Plotting

$$\frac{An}{2\,A_0} = \tfrac{1}{2}\left[1 + \mathrm{erf}\left(-\frac{x_n}{4\,Dt}\right)\right] \tag{5}$$

on gauss-arithmetic paper, a straight line of slope $-1/4Dt$ is obtained in the region where volume-diffusion occurred. This solution fits our experimental conditions and was therefore used.

Diffusion coefficients were calculated using a GE 625 Bull-General Electric computer and suitable Fortran IV programs were developed to that effect [28]. The dependence on temperature according to the Arrhenius law was verified and activation energies and frequency factors were then calculated together with the respective errors by using the least squares method [29]. This program also machine-plots the ln D versus $1/T$ curves using the computed and experimental values of D.

2.1. Materials and Procedure

Table II shows the analyses of the 99.99 wt % Zr and of the different grades of Hf which were used in the experiments. The latter only differ in the Zr content, with similar amounts of minor impurities.

TABLE II Analysis of the mean impurity contents in the materials used (ppm).

Impurity	Zr	Hf/2.7 wt % Zr	Hf/6 wt % Zr
C	6.0	60	40
N	2.1	23	26
O	25.0	180	90
H	3.3	2.5	17
Al	3.0	39	40
Si	1.5	<40	—
Ti	1.0	93	<35
Fe	30.0	245	160
W	<0.70	<20	<30
Cu	0.01	<40	<25
Ni	1.50	<10	15
Mg	<0.05	<10	<20
Mn	<0.03	<10	<20
Hf	40.00		

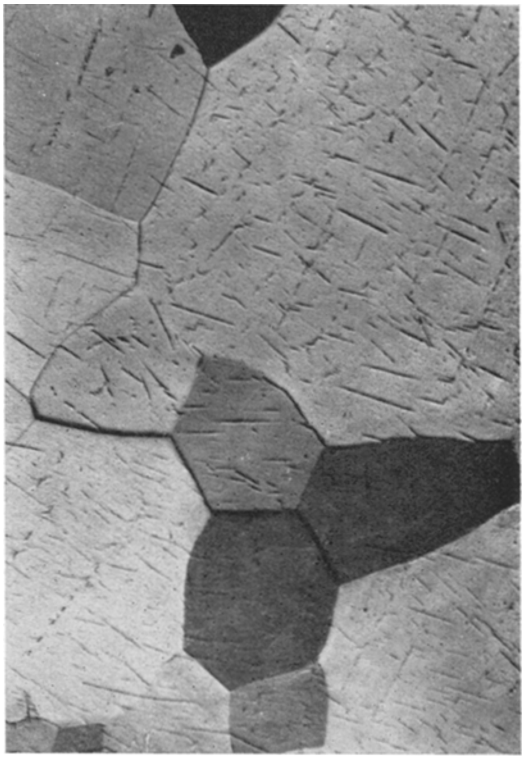

Figure 1 Typical structure of stabilised Zr (× 100).

The specimens were stabilised by long annealing treatments at temperatures just below that of transformation to the β-phase. Figs. 1 and 2 show the structure of stabilised specimens. No grain growth was observed after the diffusion-annealing.

Following a previously used technique [25], the diffusion pairs were prepared by electrolytic deposition of the radioactive tracer on the polished surface of the specimens. A mixture of $Zr^{95} + Nb^{95}$ was used as tracer for Zr and a mixture of $Hf^{175} + Hf^{181}$ for Hf.

Zirconium samples were diffusion-annealed in Chevenard-Joumier furnaces which maintained the required temperature within ±2° C. Annealing was carried out under 1.2 atm of purified argon (99.998 %).

Diffusion-annealing treatments of hafnium up to 1500° C were performed in a furnace with a platinum heating element under a similar protective atmosphere. Treatments up to 1700° C were carried out under vacuum (10^{-6} torr) in a furnace with a tantalum heating element. The temperatures, measured with Pt/Pt 10% Rh thermocouples, were recorded during all the

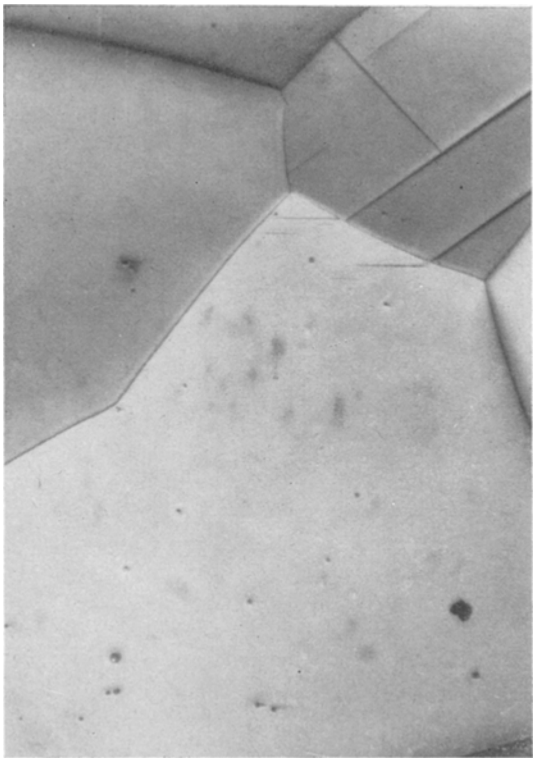

Figure 2 Typical structure of stabilised Hf 2.7 wt % Zr (× 100).

treatments. They were found to be accurate within ± 2° C for treatments up to 1200° C and within ±5° C for higher temperature.

To avoid errors due to surface-diffusion, 0.5 mm was removed from the specimen sides after the annealing treatment. As the penetration was at best of the order of 100 μm it was necessary to resort to abrasion and for that effect a rotating polishing device was designed and constructed (fig. 3). This gave a practically constant parallelism of the faces, which was checked between polishing by means of a Reischauer electromagnetic measuring apparatus. The thickness of the material removed (about 1 to 3 μm each time) was determined by weight which was measured within an accuracy of ±2 × 10^{-5}g*.

The activity measurements of Zr were carried out using a Ge/Li detector of 5 cm^3 volume and a multichannel pulse analyser of 256 channels. Under optimum conditions the resolution of the

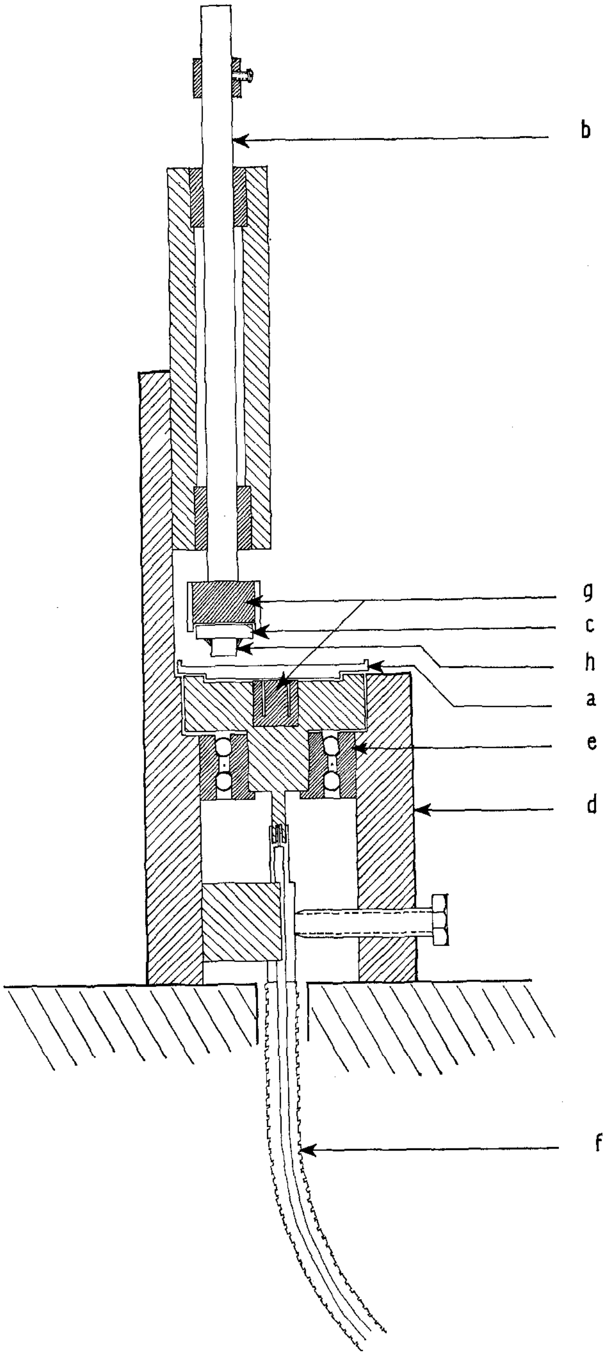

Figure 3 Rotating polishing device: (a) steel wheel and attached abrasive paper; (b) rotating guide; (c) magnetic specimen holder; (d) steel frame; (e) ball-bearing; (f) rotating shaft; (g) magnets; (h) specimen.

---

*Because of dissimilar contents of Zr, widely scattered values for the density of Hf are found in the literature [30]. Therefore we determined the density of the materials used in the present case, and obtained Hf/2.7 wt % Zr, $d = 12.92$ g/cm^3; Hf/6.0 wt % Zr, $d = 12.40$ g/cm^3.

Ge/Li detector used is of 2.5 keV for the Ga^{153} peaks (96 keV and 103 keV).

It was, therefore, possible to resolve the 726 keV and 760 keV peaks due to Zr^{95} from that of 765 keV due to Nb^{95}. Fig. 4 shows the gamma spectrum of mixture of these isobars obtained by using the Ge/Li detector.

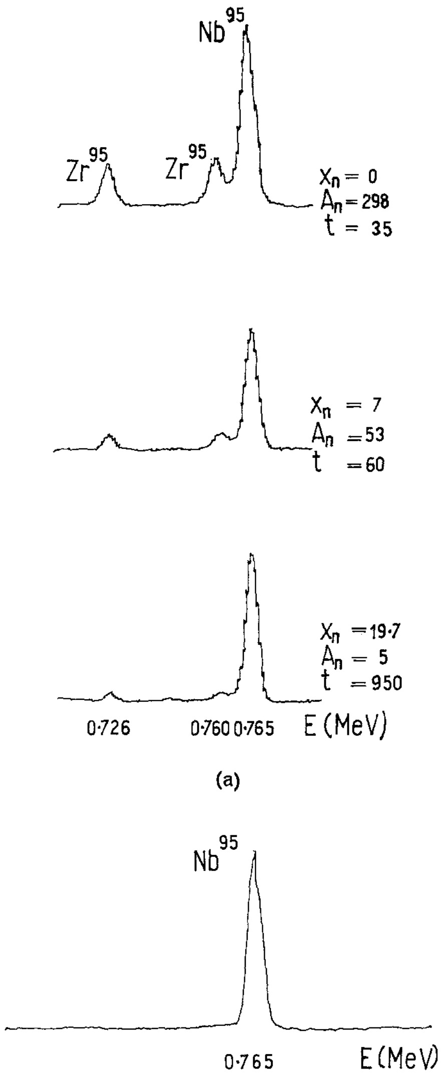

(a)

(b)

Figure 4 Gamma spectrum of Zr^{95} + Nb^{95} and Nb^{95}. (a) Typical residual activities of Zr annealed 1 month at 763° C. x_n = penetration (cm × 10^{-4}); A_n = activity measured in the 726 keV peak (n° C/min); t = counting time (min). (b) Activity of pure Nb^{95}.

Calculations were carried out as follows. (i) Self-diffusion coefficients of Zr were calculated from the activity values obtained for each penetration from the 726 keV peak due exclusively to Zr^{95}. To avoid contributions from Nb^{95} the 760 keV peak due to Zr^{95} was not considered. (ii) To check the influence of Nb^{95} and to compare our values with those obtained without Nb^{95} separation, self-diffusion coefficients of Zr were also calculated from values obtained from the total activity of the three peaks.

Fig. 4 shows the gamma spectrum of Zr^{95} + Nb^{95} as obtained by a recorder attached to the multichannel. Each graph shows the residual activity after abrasion of a Zr specimen annealed at 763° C over a month. It is noticeable that the Nb^{95} peak is higher than those which correspond to Zr^{95} and that it is still existent when the Zr^{95} peaks have disappeared. When studying these graphs it must be borne in mind that the counting time was increased (from a few minutes to several hours) with decreasing activity, in order to maintain the same statistical error. It was also necessary to use different scales. Fig. 4 shows the penetration, x_n, activity, A_n, (as measured from the 726 keV peak) and counting time, t, for each abrasion.

A separate set of experiments were carried out to find the diffusion coefficients of Nb^{95} in α-Zr. Similar experimental techniques were used and the activity of Nb^{95} was measured with a NaI (Tl) crystal. Fig. 4 shows the gamma spectrum of Nb^{95}. Results obtained from our previous measurements of the 765 keV peak would have included activity of Nb^{95} arising as a decay product of Zr^{95} and the interpretation of such values would have become unnecessarily complicated.

Fig. 5 shows a gauss-arithmetic plot of penetration curves of Zr^{95} and Nb^{95} after 18 days of diffusion-annealing at 795° C.

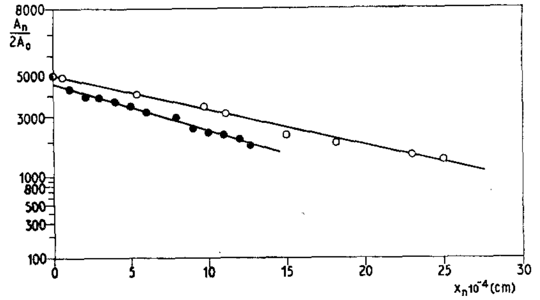

Figure 5 Activity profiles for diffusion of Zr^{95} (●) and Nb^{95} (○) in hcp Zr.

Hf activities were measured with a NaI (Tl) detector and a single channel spectrometer. It was not possible to consider the isotopic effect (table III) which, at any rate, lies within the experimental error. Fig. 6 shows the Hf^{175} + Hf^{181} gamma spectrum as resolved with a Ge/Li detector. Fig. 7 shows gauss-arithmetic plots of $A_n/2A_0$ versus x_n for Hf 2.7 wt % Zr annealed at 1300° C for 4 days and for Hf 6 wt % Zr annealed at 1537° C for 3 h.

TABLE III

Radioisotope	Hf^{175}		Hf^{181}	
Half-life	70 days		45 days	
Production	Hf^{174} (n, γ)	Hf^{175}	Hf^{180} (n, γ)	Hf^{181}
Decay	Hf^{175} $\xrightarrow{\beta^+}$	Lu^{175}	Hf^{181} $\xrightarrow{\beta^-}$	Ta^{181}
	$\Downarrow$		$\Downarrow$	
Radiation emitted	C.E.	γ	β	γ
Energy (MeV)	0.34	0.089	0.41	0.133
	0.43	0.114		0.136
	0.50	0.161		0.346
		0.230		0.482
		0.343		
		0.433		

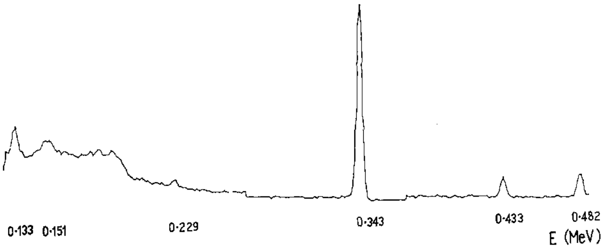

Figure 6 Gamma spectrum of $Hf^{175}+Hf^{181}$ obtained with a Ge/Li detector.

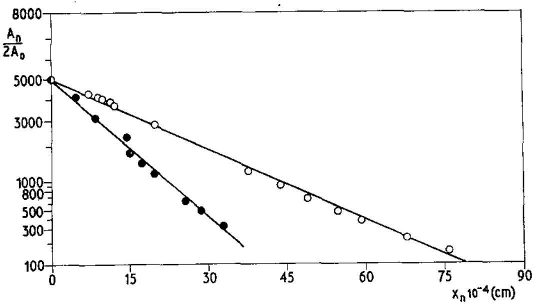

Figure 7 Activity profiles for diffusion of $Hf^{175}+Hf^{181}$ in Hf/2.7 wt % Zr (●) and Hf/6 wt % Zr (○) in hcp phase.

3. Results

Tables IV and V give the values of diffusion coefficients obtained from the various experiments. Graphs of ln D versus $1/T$ for α-Zr and α-Hf are respectively shown in figs. 8 and 9.

TABLE IV Diffusion coefficients obtained for Zr^{95}, Zr^{95} + Nb^{95}, and Nb^{95}.

T	$t \times 10^{-6}$	D (cm²/sec)		
(° C)	(sec)	Zr^{95}	Zr^{95} + Nb^{95}	Nb^{95}
857	1.1088	1.2×10^{-12} 1.3×10^{-12}	2.8×10^{-12}	5.3×10^{-12}
830	1.5492	7.8×10^{-13}		4.1×10^{-12}
795	1.6356	7.2×10^{-13}	1.6×10^{-12}	2.1×10^{-12}
763	2.6658	4.0×10^{-13} 3.9×10^{-13}		
740	2,6199		8.9×10^{-13}	1.1×10^{-12}

TABLE V Self-diffusion coefficients for Hf.

Hf/2.7 wt % Zr			Hf/6 wt % Zr		
T (° C)	$t \times 10^{-5}$ (sec)	D (cm²/sec)	T (° C)	$t \times 10^{-4}$ (sec)	D (cm²/sec)
1483	0.144	3.4×10^{-11}	1689	1.4400	3.1×10^{-10}
1470	0.261	5.8×10^{-11}	1651	0.9000	2.0×10^{-10}
1373	1.68	1.4×10^{-11}	1550	2.1600	1.2×10^{-10}
1350	3.1248	1.8×10^{-11}	1537	1.0493	1.4×10^{-10}
1300	3.492	1.6×10^{-11}	1420	1.4760	5.6×10^{-11}
1270	0.936	8.6×10^{-12}			
1120	1.500	2.8×10^{-12}			
1120	1.500	3.8×10^{-12}			
924	16.354	1.5×10^{-13}			
924	16.354	1.5×10^{-13}			

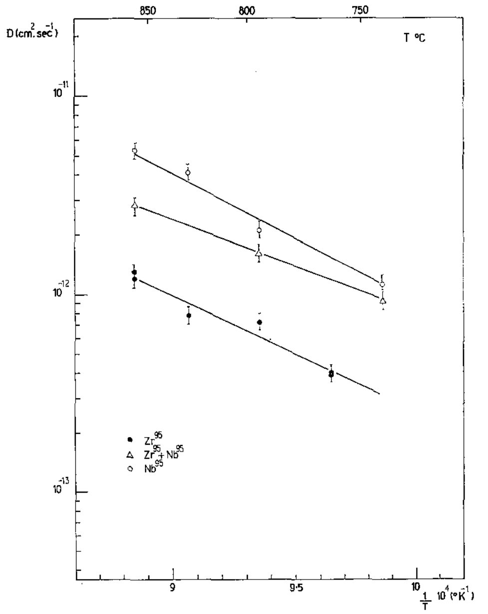

Figure 8 Temperature dependence of diffusion of Zr^{95}, Zr^{95} + Nb^{95}, and Nb^{95} in hcp Zr.

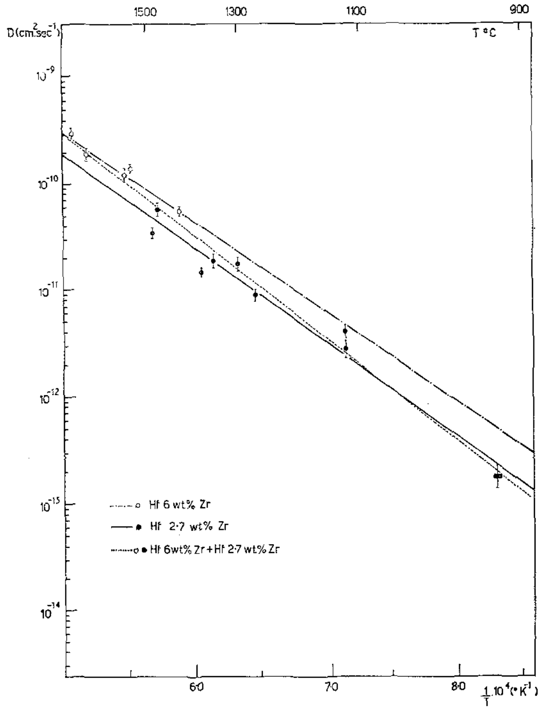

Figure 9 Temperature dependence of diffusion of Hf^{175} + Hf^{181} in hcp Hf.

Table VI gives the values of Q and D_0 obtained in each case, together with the error in Q and ln D_0 obtained by the least squares method.

From these results the following can be concluded.

(*a*) The difference between values of Q and D_0 for diffusion of Zr^{95} + Nb^{95} and self-diffusion of Zr^{95} is larger than the experimental error. It is therefore convenient to eliminate the influence of Nb^{95} in activity measurements if Zr self-diffusion constants are to be correctly measured.

(*b*) The rate of diffusion of Nb^{95} in Zr is slightly higher than that of self-diffusion of Zr^{95}. The differences in Q and D_0 however lie within the experimental error, meaning that a neat diffusion separation of the two isobars cannot be obtained by diffusion. On the other hand, their half-lives are similar (table I) and secular equilibrium conditions are not easily attained. Thus, no activities due exclusively to Zr^{95} can be measured if it has not been chemically separated or the different radiations resolved by means of a suitable detector.

(*c*) No other values for diffusion of Nb^{95} in α-Zr are known to the authors. However Lundy and Federer [7], for the diffusion of Zr^{95} and Nb^{95} in β-Zr, found that the variation of ln D versus $1/T$ does not follow an Arrhenius law. They suggest that Q and D_0 are temperature-dependent and they obtained the apparent activation energies as a linear function of temperature and the pre-exponential terms as a power function of the absolute temperature.

It is not valid to calculate values of Q and D_0 in the α-phase range of temperature from the formulae obtained by them. It can be pointed out however that for both phases the values of D_0 (Zr) and Q (Zr) are smaller than those of D_0 (Nb) and Q (Nb) but the diffusivity of Zr^{95} is greater than that of Nb^{95} in the β-phase.

(*d*) Values presented here and those obtained by other investigators are compared in table VII and fig. 10. There is a close agreement between our values for Zr^{95} + Nb^{95} and those obtained by Gruzin [21] and Borisov [22]. They do not agree with those obtained by Lyashenko [23], which are nearer to those predicted by current semi-empirical equations.

Flubacher [24] measured Zr^{95} exclusively, but his values do not agree with ours, probably because (i) his separation of Nb^{95} was not 100% effective; (ii) grain growth in the non-stabilised α-phase materials somehow influenced the diffusion process.

We have calculated, from Flubacher's data, the following values for his stabilised and non-stabilised 99.95 wt % Zr for the same purity as used by him.

	Q (cal/mole)	D_0 (cm^2/sec)
non-stabilised Zr	48600 ± 4300	2.6×10^{-3}
stabilised Zr	39300 ± 3800	3.5×10^{-5}

The values for stabilised material decrease

TABLE VI

	Q (cal/mole)	D_0 (cm^2/sec)	ln D$_0$	Standard Deviations ln D$_0$	 Q
Zr^{95} in Zr	27000	2.1×10^{-7}	−15.395	1.923	2900
Zr^{95} + Nb^{95} in Zr	22200	5.5×10^{-8}	−16.715	0.280	420
Nb^{95} in Zr	31500	6.6×10^{-6}	−11.934	1.800	2700
Hf^{175} + Hf^{181} in Hf/2.7 wt % Zr	41600	7.3×10^{-6}	−11.822	1.122	2300
Hf^{175} + Hf^{181} in Hf/6 wt % Zr	39100	6.4×10^{-6}	−11.965	1.696	4400

TABLE VII

Ref. and author	T range (° C)	Purity (wt %)	Method*	Zr^{95} + Nb^{95}		Zr^{95}	
				Q (cal/mole)	D_0 (cm²/sec)	Q (cal/mole)	D_0 (cm²/sec)
[21] Gruzin *et al*	300-700	99.96	R.A.	22000	10^{-7}		
[22] Borisov *et al*	700-800	99.96	R.A.	22000	5×10^{-8}		
[23] Lyashenko *et al*	650-825	99.96	R.A.	52000	5.9×10^{-2}		
[24] Flubacher	750-850	99.90 99.95	S.S.			45500	5.6×10^{-4}
This work	740-857	99.99	R.A.	22200	5.5×10^{-8}	27000	2.1×10^{-7}

*R.A. = residual activity; S.S. = serial sectioning

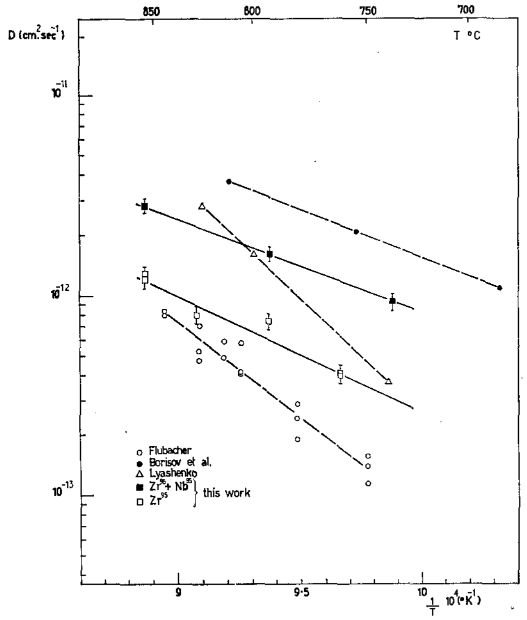

Figure 10 Comparison of present results with results obtained by other investigators on self-diffusion of Zr.

and tend towards our still lower values. The difference may arise from the dissimilar techniques used.

(*e*) Q and D_0 were separately calculated for both qualities of Hf used. The difference between them is smaller than the experimental error and therefore, nothing can be said about the influence of Zr, in this range of composition. Furthermore, using the whole set of results, the linear approximation still holds (as shown by the dotted line in fig. 9) and Q and D_0 values are similar to those mentioned above. However, values of D for 6 wt % Zr content are slightly higher than those for 2.7 wt % Zr*.

3.1. Error Evaluation

Considering the following sources of error, a total error of the order of 10% has been estimated for the values of diffusion coefficient. (i) Error in measurements of the thickness of material removed in each abrasion, $\epsilon(x_n) \simeq 3\%$; (ii) error due to the faces not being parallel, negligible; (iii) error in annealing time, negligible; (iv) error in activity measurements, $\epsilon(A_n) \simeq 1\%$, which gives an average error in the argument of the error function $\epsilon(u) \simeq 2\%$.

4. Discussion and Conclusions

The experimental and semi-empirical values of Q and D_0 and activation entropies are compared in table VIII for the IV-A group elements which have a hcp phase stable at low temperature.

For the calculation of ΔS, the parameter λ which accounts for crystalline structure in Zener's equation [33], $\Delta S = \lambda\theta Q/Tm$, was estimated from data existing for hcp metals [34]. It varies between 0.9 and 2.2 and this does not significantly affect the differences between ΔS_{theor} and ΔS_{exp}. θ has been determined for all three elements [35-37].

The melting points which would correspond to the α-phase of Ti and Zr have been calculated by Ardell [38] and Kaufman [39]. Similar calculation for Hf is not possible since thermodynamic data are not complete. The normal melting point was used, as the expected differences are not large and should not influence the results significantly.

*This suggests the following considerations. Since the Zr atomic radius is 0.7% larger than that of Hf, internal strains may arise from the presence of Zr in the lattice. These strains may relax by the creation of extrinsic vacancies, which may account for the higher diffusivity of Hf/6 wt % Zr. This assumes the operation of a vacancy mechanism, which, even if largely accepted, is far from proved for the present case. The presence of extrinsic vacancies can be determined by density measurements and X-ray measurements of lattice parameter (to determine the theoretical density). The experimental difficulties are, however, considerable.

TABLE VIII Self-diffusion characteristics of h.c.p. phases.

		Q (cal/mole)				ΔS (cal/mole °K)	
Element	Tm (° K)	Q_{exp}	$Q = 35T\text{m}$ [31]	$Q = \text{R}T\text{m}$ (K + 1, 5V) [1]	$Q = \frac{700}{\alpha}$ [32]	ΔS_{exp}	Δ_{theor}
Ti* 99.99 wt %	1730	35900	60500	68700	63600	−14	22
Zr 99.99 wt %	1858	27000	65000	79300	97200	−21	15
Hf 2.7 wt % Zr	2495	41600	87300	106500	127200	−14	13

*D_0 for self-diffusion of Ti is: 8.6×10^{-6} cm²/sec

It should be pointed out here that the present values of Q and D_0 for α-Ti differ slightly from those published previously [25]. Former values were obtained from 99.89 wt % pure Ti and calculation done using equation 2 from Gruzin's method. The derivative $\partial A/\partial x$ was obtained graphically. The new set of experiments was performed on 99.99 wt % pure Ti, and calculations were made by a computer, using equation 3, consequently diminishing the error of D. Reprocessing the old and some new data from 99.89 wt % Ti we found the results agreed within experimental error with the new values for 99.99 wt % Ti. No impurity effect was, therefore, detected.

From these results we observe the following. (i) The activation energies have approximately half the values predicted by semi-empirical relationships based on physical properties (table VIII). (ii) The frequency factors D_0 lie quite apart from the usual band of values (i.e. 0.01 to 10 cm²/sec), and their values are too small to satisfy Zener's theory; when interpreted according to a vacancy model they give negative activation entropies. (iii) Arrhenius' law is followed in all instances, implying the operation of a single diffusion mechanism over the whole temperature interval. Due to its high allotropic transformation temperature, the temperature interval for Hf is particularly large.

Amongst hcp metals studied so far, Ti, Zr and Hf are the only ones which do not obey the semi-empirical rules based on experimental data. Their study becomes the more interesting since they also show abnormal behaviour in the β-(bcc) phase.

Curved ln D versus $1/T$ plots have been obtained by some authors for β-Ti [3] and β-Zr [7], but Libanati and de Reca [2] have shown that β-Ti and β-Hf obey Arrhenius' law with anomalous Q and D_0 values, as above.

Table IX shows that, within the experimental error, the activation energies of the three elements have similar values for both phases. The relationship between $D_0(\alpha)$ and $D_0(\beta)$ is approximately the same for the three elements,

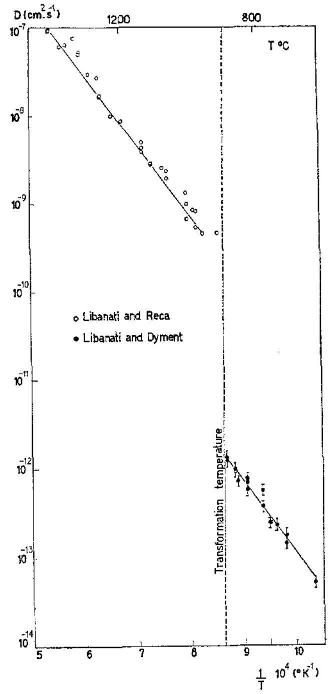

Figure 11 Temperature dependence of diffusion of Ti^{44} in hcp and bcc Ti.

TABLE IX

	Q (cal/mole)		D_0 (cm²/sec)		
Element	α phase	β phase	α phase	β phase	$D_0(\alpha)/D_0(\beta)$
Ti	35900	36500	8.6×10^{-6}	1.9×10^{-3}	0.452×10^{-2}
Zr	27000	27700	2.1×10^{-7}	8.5×10^{-5}	0.247×10^{-2}
Hf	41600	43800	7.3×10^{-6}	4.8×10^{-3}	0.152×10^{-2}

although the order of magnitude of the values of $D_0(\alpha)$ and $D_0(\beta)$ for Zr is different from those for Ti and Hf. For β-Ti and β-Hf we have used Libanati and de Reca's results; for β-Zr, assuming that two diffusion mechanisms operate, we have used Q and D_0 values corresponding to the low temperature range, as calculated by Kidson [14] from their own results and those of Lundy and Federer [7]. Figs. 11 to 13 show ln D versus $1/T$ for Ti, Zr and Hf in the α- and β-phases.

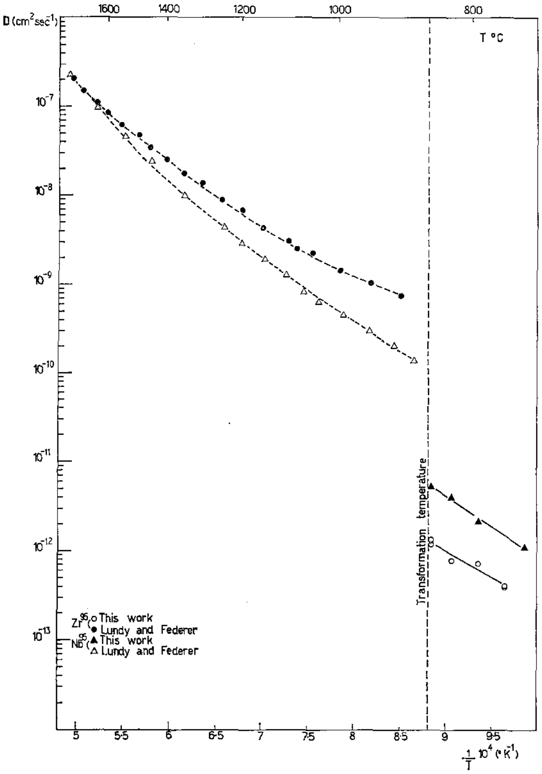

Figure 12 Temperature dependence of diffusion of Zr^{95} and Nb^{95} in hcp and bcc Zr.

This suggests that, if two diffusion mechanisms operate in the β-phase, the low temperature one also operates in the α-phase. If, on the other hand, a single mechanism operates in the β-phase, it is the same one as operates in the α-phase.

This makes us think that the anomalies in diffusion behaviour hitherto regarded as characteristic only of a bcc structure may be somehow a characteristic of this group of elements.

Hf offers, among the elements belonging to group IV-A, the possibility of investigation of the operating mechanism by measuring the isotopic effect using Hf^{175} and Hf^{181}. An appropriate detector and very refined techniques are required and we intend to present some results in this line in the near future.

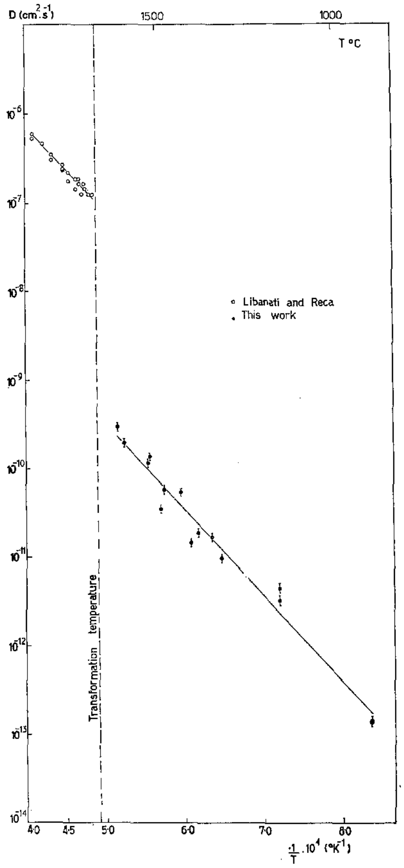

Figure 13 Temperature dependence of diffusion of Hf^{175} + Hf^{181} in hcp and bcc Hf.

Acknowledgements

This work has been partly performed with the economical assistance of the Consejo Nacional de Investigaciones Científicas y Técnicas (subsidy no. 2185). We are also grateful to Lic. D. Fainstein for very helpful discussion.

References

1. A. D. LE CLAIRE in "Diffusion in BCC Metals" (Amer. Soc. Metals, 1965) p. 3.
2. N. W. DE RECA and C. M. LIBANATI, *Acta Met.*, to be published.
3. J. F. MURDOCK, T. S. LUNDY, and E. E. STANSBURY, *ibid* **12** (1964) 1033.
4. R. F. PEART, D. GRAHAM, and D. H. TOMLIN, *ibid* **10** (1962) 123.

5. G. B. Gibbs, D. Graham, and D. H. Tomlin, *Phil. Mag.* **8** (1963) 1269.
6. D. Graham in "Diffusion in BCC Metals" (Amer. Soc. Metals, 1965) p. 27.
7. J. I. Federer and T. S. Lundy, *Trans. Met. Soc. AIME* **227** (1963) 592.
8. G. V. Kidson, *Canad. J. Phys.* **41** (1963) 1563.
9. D. Volokoff, S. May, and Y. Adda, *Compt. rend.* **251** (1960) 2341.
10. T. S. Lundy, Oak Ridge Report (USA) ORNL 3617 (June, 1964).
11. S. J. Rothman, L. T. Lloyd, R. Weil, and A. L. Harkness, *Trans. Met. Soc. AIME* **218** (1960) 605.
12. S. J. Rothman and N. L. Peterson in "Diffusion in BCC Metals" (Amer. Soc. Metals, 1965) p. 183.
13. F. R. Winslow and T. S. Lundy. *Trans. Met. Soc. AIME* **233** (1965) 1790.
14. G. V. Kidson in "Diffusion in BCC Metals" (Amer. Soc. Metals, 1965) p. 329.
15. G. B. Gibbs, *Acta Met.* **12** (1964) 1302; *idem, Mem. Sci. Rev. Met.* **62** (1965) 841; J. Askill and G. B. Gibbs, *Phys. Stat. Solidi* **11** (1965) 557; G. B. Gibbs, *Acta Met.* **15** (1967) 1551.
16. G. Pound, W. Bitler, and H. Paxton, *Phil. Mag.* **6** (1961) 473.
17. E. W. Hart, *Acta Met.* **5** (1957) 597.
18. A. J. Mortlock, *ibid* **8** (1960) 132.
19. M. C. Naik and R. P. Agarwala, *ibid* **15** (1967) 1521.
20. F. Dyment, D. Fainstein, and C. M. Libanati, *Scripta Met.*, to be published.
21. P. L. Gruzin, V. S. Emelyanov, G. Riabova, and G. B. Fedorov, 2nd UN International Conf. for Peaceful Uses of Atomic Energy, **19** (1958) 187.
22. E. V. Borisov, Yu G. Godin, P. L. Gruzin, A. I. Yevstyukin and V. S. Emelyanov, *Metall. Metallov. Izdatel'stvo Akad. Nauk. SSSR* (1958) 196; Isotopes Utilisation Conf. (Moscow, 1958) p. 291.
23. V. S. Lyashenko, B. N. Bikov, and L. V. Pavlinov, *Phys. Metall. Metallov.* **8** (1959) 362.
24. P. Flubacher, EIR-Bericht no. 49 (1963).
25. C. M. Libanati and F. Dyment, *Acta Met.* **11** (1963) 1263.
26. G. Seibel, thesis, Université de Paris (1962).
27. P. L. Gruzin. *Doklady Akad. Nauk SSSR* **86** (1952) 289.
28. F. Dyment, to be published.
29. P. G. Guest, "Numerical Methods of Curve Fitting" (Cambridge University Press, Cambridge, 1961).
30. "The Metallurgy of Hafnium", edited by D. E. Thomas and E. T. Hayes (U.S. Atomic Energy Commission, 1960).
31. J. van Liempt. *Z. Physik* **96** (1935) 534.
32. J. Askill, *Phys. Stat. Solidi* **11** (1965) K49.
33. C. Zener, "Imperfections in Nearly Perfect, Crystals", edited by Schockley, Hollomon, Maurer and Seitz (Wiley, New York, 1952) p. 289.
34. Y. Adda and J. Philibert, "La Diffusion dans les Solides" (Presses Universitaires de France, Paris, 1966) p. 1132.
35. W. Köster, *Z. Metalk.* **39** (1948) 1.
36. P. E. Armstrong and H. L. Brown, Los Alamos Sci. Lab. Report (1963).
37. J. C. Crespi (Comisión Nacional de Energía Atómica, Avenida del Libertador 8250, Buenos Aires, Argentina) private communication.
38. A. J. Ardell, *Acta Met.* **11** (1963) 591.
39. L. Kaufman, *ibid* **7** (1959) 575.